An Investigation of Cross-Phase Modulation and Machine Learning Based Alleviation of Nonlinear Effects in a DP-QPSK Based DWDM System

M. N. Mahalakshmi
Department of Electronics & Telecommunication Engineering, RV College of Engineering, Visvesvaraya Technological University, India
mahalakshmimn@rvce.edu.in (corresponding author)

G. Sadashivappa
Department of Electronics & Telecommunication Engineering, RV College of Engineering, Visvesvaraya Technological University, India
sadashivappag@rvce.edu.in

Received: 10 September 2025 | Revised: 25 September 2025 and 13 January 2026 | Accepted: 14 January 2026

 DOI: https://doi.org/10.48084/etasr.14652

ABSTRACT

Dense Wavelength Division Multiplexing (DWDM) systems with Dual-Polarization Quadrature Phase-Shift Keying (DP-QPSK) technology are enabling current optical fiber communication systems in Metropolitan Area Networks and Long-haul networks. The impact of the nonlinear impairments caused by the Kerr effect is more detrimental to the performance of DWDM systems. Among these impairments, the dominant impairment is Cross-Phase Modulation (XPM). In this paper, a nine-channel coherent DP-QPSK DWDM system with Standard Single Mode Fiber (SSMF) at a bit rate of 112 Gb/s per channel is simulated in OptiSystem v18. The study examines how XPM affects performance, specifically focusing on polarization crosstalk and phase noise for different channel spacings and transmission distances up to 900 km. The alleviation of nonlinear effects is demonstrated using two Machine Learning (ML) models: Bidirectional Long Short-Term Memory (Bi-LSTM) and Transformer. The efficacy of these machine learning techniques in mitigating nonlinear effects is evaluated against Digital Back Propagation (DBP). The findings demonstrate that the Transformer model outperforms both DBP and Bi-LSTM.

Keywords-Cross-Phase Modulation; DP-QPSK; DWDM; nonlinear effects

I. INTRODUCTION

DP-QPSK-based DWDM systems provide the growing demand for bandwidth for voice, video, and high-speed data services in long-haul applications. Higher input launch power and denser grid allocation are required to enhance system capacity. But they introduce various nonlinear effects into the system. These nonlinearities degrade the signal quality to the point that even a high Optical Signal-to-Noise Ratio (OSNR) cannot restore it. Kerr-effect-driven nonlinearities, such as Four-Wave Mixing (FWM) and XPM, significantly impair system performance and limit Achievable Information Rates (AIR). Advanced modulation formats can improve spectral efficiency and data rate, but their performance is limited by phase noise. Compensating for impairments using powerful programmable Digital Signal Processing (DSP) at the receiver has significantly contributed to achieving greater reach and information rates. XPM significantly affects the system when the number of channels is large. It increases the signal spectrum width, necessitating a wider optical filter bandwidth at the receiver. A straightforward method for canceling nonlinear polarization crosstalk using a feed-forward digital signal-processing approach was proposed [1]. An analytical fiber model based on a Volterra expansion was proposed to determine the impact of XPM, accounting for the autocorrelation and variance of phase noise and polarization crosstalk, in a direct- and coherent-detection DP-QPSK-based DWDM system [2].

In this paper, the authors used Jones space analysis to incorporate both polarization scattering and phase noise. Closed-form formulas were derived for crosstalk caused by Self Phase Modulation and XPM in a one-span Wavelength Division Multiplexing (WDM) system with Distributed Raman Amplifiers [3]. The authors examined how Equalization Enhanced Phase Noise (EEPN) affects Bit Error Rate (BER) performance and AIR in a super channel Nyquist-spaced system, employing DBP across multiple channels and

Electrical Dispersion Compensation (EDC) [4]. A Decision-Feedback Nonlinear Polarization Crosstalk Canceler (DF-NPCC) was proposed to mitigate nonlinear effects [5]. A nonlinear model suitable for asymmetric and arbitrary modulation formats was proposed [6]. In a multichannel environment, the aggregate phase noise and polarization crosstalk induced by XPM comprise the cumulative effects across all co-propagating channels, as demonstrated in references [7, 8]. Presently, dispersion compensation is managed using DSP at the receiver side. The crosstalk impact is much more detrimental than the nonlinear interaction of Amplified Spontaneous Emission (ASE) noise and signal [9]. The differential Evolution optimization algorithm contributed to obtaining fibers with low dispersion and required optical parameters [10]. The performance of a DWDM system was studied for varying numbers of channels, amplification sections, and transmission rates [11]. Because DBP is constrained by its computational overhead, attention has shifted to ML-based techniques to alleviate nonlinear effects. Several studies have reported the use of Neural Networks (NN) [12] [13], Support Vector Machines (SVM) [14], and clustering techniques [15]. A transformer-based method for nonlinear compensation in a long-haul DP-16 Quadrature Amplitude Modulation (QAM) single-channel communication system was demonstrated [16]. Constellations were optimized using geometric shaping for single-span systems [17].

The contributions of the paper are as follows:

- Investigated the impact of XPM on a multichannel, 112Gbps coherent DP-QPSK-based DWDM system that enables current optical fiber communication systems in Metropolitan Area Networks and Long-haul networks.
- Incorporated Machine Learning models at the receiver to alleviate nonlinearities. The performance of these ML techniques is compared with that of the DBP algorithm across different transmission distances.
- The results obtained show that ML techniques will provide a promising solution for alleviating nonlinear effects in multichannel systems.

II. THEORETICAL BACKGROUND

The impact of XPM is reflected in two phenomena: phase noise and polarization scattering. The coupled Manakov equations were used by the authors to model these phenomena [2, 5]. Here $u_{1x/y}$ and $u_{2x/y}$ are the optical fields of polarization x/y of both the channel interest and the channel which is causing interference. γ is the coefficient of nonlinearity, α is the loss of fiber, β_2 denotes Group Velocity Dispersion. The starting terms on the right-hand side of (1) and (2) signify (Self-Phase Modulation) SPM, and the second term signifies XPM. The third term represents polarization crosstalk. As shown in [2], the polarization crosstalk and phase noise resulting from XPM can be determined using equations (3) and (4), where $w_{yx/xy}$ is the polarization crosstalk and $\oint_{x/y}$ is the phase noise. In (5), $H_{m,n}(\omega)$ denotes the XPM filter, m stands for channel index and n indicates the span number and $u_{m,x/y,n}$ is the interfering channel waveform.

$$\frac{\partial u_{1x/y}}{\partial z} + \frac{\alpha}{2} u_{1x/y} + j\frac{\beta_2}{2}\frac{\partial^2 u_{1x/y}}{\partial t^2} = j\frac{8}{9}\gamma\,[(|u_{1x/y}|^2 + |u_{1y/x}|^2)\,u_{1x/y} + (2|u_{2x/y}|^2|u_{2y/x}|^2)\times u_{1x/y} + u_{2x/y}\,u^*_{2y/x}u_{1y/x}] \quad (1)$$

$$\frac{\partial u_{2x/y}}{\partial z} + \frac{\alpha}{2} u_{2x/y} + d\frac{\partial u_{2x/y}}{\partial t} + j\frac{\beta_2}{2}\frac{\partial^2 u_{2x/y}}{\partial t^2} = j\frac{8}{9}\gamma[(|u_{2x/y}|^2 + |u_{2y/x}|^2)\,u_{2x/y} + (2|u_{1x/y}|^2 + |u_{1y/x}|^2)\times u_{2x/y} + u_{1x/y}\,u^*_{1y/x}u_{2y/x}] \quad (2)$$

$$w_{yx/xy} = \sum_{m=2}^{M}\sum_{n=1}^{N} j\,u_{m,x/y,n}\left(0, t-\tau_{m,n}\right)u^*_{m,y/x,n}\times\left(0, t-\tau_{m,n}\right)h_{m,n}(t) \quad (3)$$

$$\oint_{x/y} = \sum_{m=2}^{M}\sum_{n=1}^{N} 2\,|u_{m,x/y,n}\left(0, t-\tau_{m,n}\right)|^2 + \left|u_{m,x/y,n}\left(0, t-\tau_{m,n}\right)\right|^2 \otimes h_{m,n}(t) \quad (4)$$

$$H_{m,n}(\omega) = \frac{8\gamma_n}{9}\,\frac{1-\exp(-\alpha_n L_n + j\Delta\beta'_{m,n}\omega L_n)}{\alpha_n - j\Delta\beta'_{m,n}\omega} \quad (5)$$

III. METHODOLOGY AND EXPERIMENTAL SET UP

The schematic of the simulated DWDM system is shown in Figure 1. The visual representation of the simulated nine-channel DWDM system is shown in Figure 2. The system is simulated using Optisystem V.18. Table I shows the system parameters. As shown in Figure 2, nine distinct channels, each with a 112 Gbps data rate, are multiplexed to achieve a 1 Tbps optical link. The system is simulated for channel spacings of 100 GHz, 50 GHz, and 25 GHz. The middle channel (Ch. 5) is used as the probe channel at a power of -3 dBm. All other channels have a launch power of +3 dBm. The optical amplifier produces ASE noise. This noise is ignored in this study. DP-QPSK is a sophisticated digital modulation technique used primarily in optical communication. The Pseudo Random Bit Sequence (PRBS) generator on each channel produces information at 112 Gbps. In the DP-QPSK transmitter, the photonic signal from a continuous-wave laser is divided into two orthogonal polarization components, which are then modulated separately by two quadrature modulators to yield X-polarized and Y-polarized signals. The PSK sequence generators create M-ary symbols from the incoming signal and send them to the M-ary pulse generators.

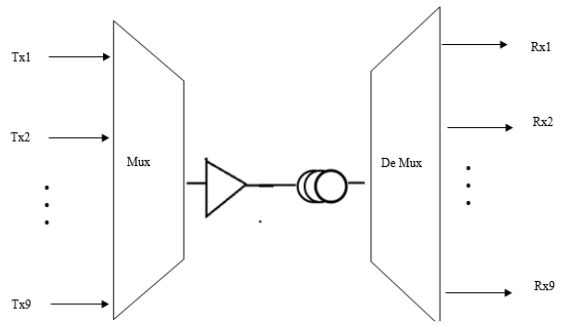

Fig. 1. Schematic diagram of the DWDM system.

The outputs of quadrature modulators are combined with a perpendicular polarization state using a polarization beam

combiner to produce a DP-QPSK signal. This signal is transmitted over the fiber. An SSMF without inline dispersion compensation is used for transmission. An optical amplifier is used before launching the signal onto the fiber to compensate for fiber attenuation. Polarization Mode Dispersion (PMD) group delay is kept minimum and constant at 0.05 ps/km$^{1/2}$. At the front end of the receiver, a 4th-order Gaussian optical bandpass filter is used to emphasize the main lobe of the spectrum, thereby avoiding unnecessary frequencies from the transmitter and channel. The received signal at the fiber end is independently demodulated by two PSK receivers operating on a single polarization. In the DP-QPSK receiver, the signal's two polarization components are combined with the local oscillator signal.

TABLE I. SYSTEM PARAMETERS

Parameter	Value
Wavelength of transmission	1546.118nm to 1552.52nm (C band)
No. of channels	9
Bit rate	112 Gbps per λ
Distance of transmission	Upto 900km
Baud rate	28GBd
Launching power	-3 dBm to +3dBm
Line width of the LASER	0.1MHz
Type of optical fibre	SSMF
Effective area of fibre (Aeff)	76.02 -76.47µm2
Fibre attenuation (α)	0.1892dB/km
Fibre dispersion	18.92ps/nm/km
PMD differential group delay	0.05ps/km1/2
Channel spacing	100GHz, 50GHz, 25GHz
Photodiode	InGaAs PIN
Responsivity of photodiode	1 A/W

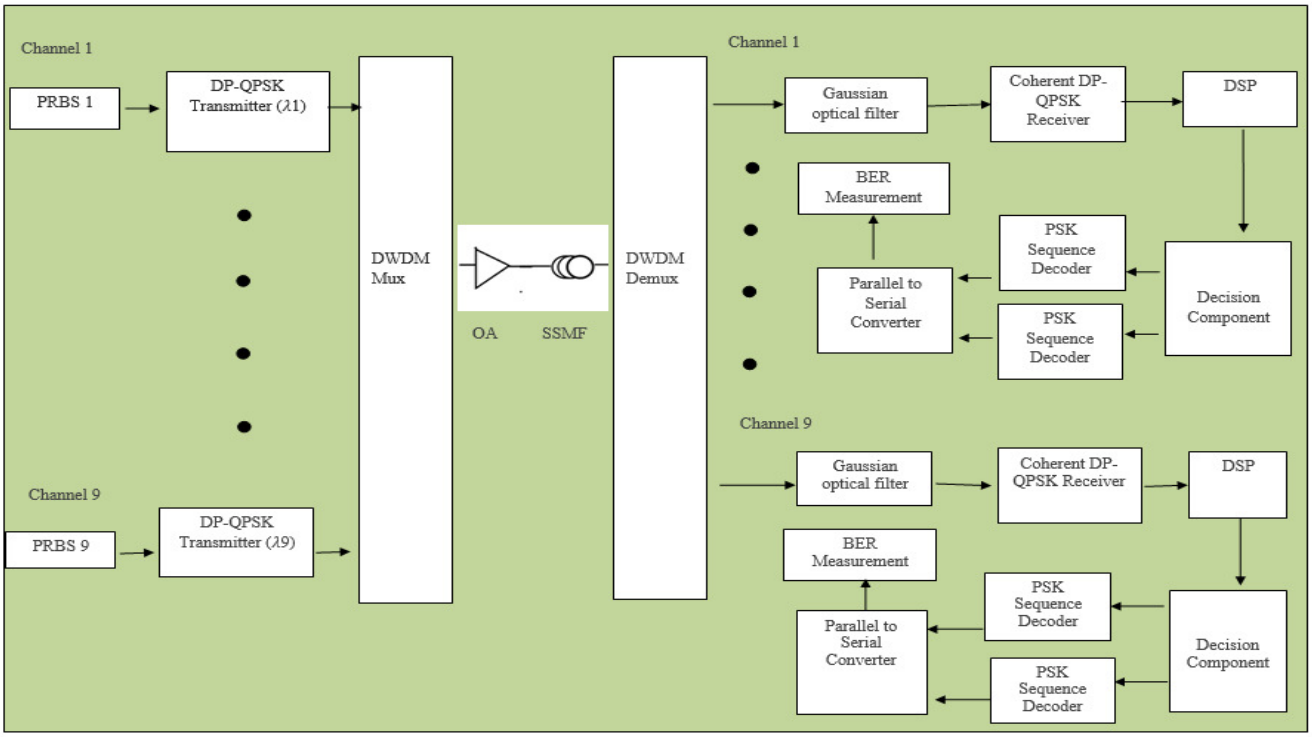

Fig. 2. Schematic diagram of nine channel DWDM system using DP-QPSK.

Combining is performed at the directional 3-dB coupler, along with a phase shift of 90^0. The outgoing signal of the coupler is directed onto two similar p-i-n photodiodes to bring out two photo currents, which are then subtracted and amplified by Electronic Amplifiers (EA) to form the output I-phase and Q- phase photocurrents. These photocurrents are fed to the DSP. The algorithms that run inside the DSP are (i) Filtering (ii) Resampling (iii) Quadrature Imbalance compensation (iv) Chromatic Dispersion (CD) compensation (v) Non Linear Effects compensation (vi) Frequency Offset Estimation (vii) Carrier Phase Estimation. Inside the DSP block, filtering focuses on the principal lobe of the spectrum. A Bessel filter is employed here to remove band noise. Upsampling is performed to elevate the sampling rate. Imperfections within the optical hybrid and balanced receiver give rise to Quadrature Imbalance (QI). In this context, QI compensation is performed using Gram-Schmidt orthogonalization to correct phase and amplitude discrepancies between the in-phase and quadrature-phase signals. CD is mitigated through digital filtering in the frequency domain. Subsequently, DBP is employed to diminish nonlinear effects. Mixing the local oscillator signal with the received signal affects the frequency and phase offsets. This Frequency Offset (FO) is estimated by maximizing the periodogram. To reduce residual CD, Adaptive Equalization (AE) using the Constant Modulus Algorithm is employed. Carrier phase recovery is conducted using the blind phase search algorithm. The Decision component initially normalizes the amplitudes of the In-phase and Quadrature-phase channels

to align with the QPSK grid and subsequently performs a decision on each received symbol by comparing it to normalized threshold levels. The two parallel M-ary PSK symbol sequences are decoded into binary signals by a PSK sequence decoder. These parallel binary sequences are converted into a single binary sequence by a parallel-to-serial converter, which then feeds it into the BER measurement device.

IV. SIMULATION RESULTS

A. Investigation of XPM

Phase noise resulting from XPM increases bit errors. The phase noise generated by the LASER at both the transmitter and the receiver is minimized to isolate phase noise caused by XPM alone. Polarizations across all channels are uniformly aligned. The power injected into the probe channel ch5 is -3 dBm. All other channels are interfering channels with a launch power of +3 dBm, used to evaluate the impact of XPM on the probe channel. A channel spacing of 100 GHz is maintained between successive channels. The phase noise and crosstalk variations influenced by XPM are measured. BER is recorded for transmission distances ranging from 100 km to 900 km by counting the number of error bits. The Q factor in decibels (dB) is computed using equation (6). The phase noise variance for the signal on the capping X polarization is measured using an optical spectrum analyzer with a normalized bandwidth of 1 Hz. Additionally, the polarization crosstalk within the system is quantitatively assessed using equation (7).

$$Q = 20\, log_{10}\left[\sqrt{2}\, erfc^{-1}(2BER)\right] \quad (6)$$

$$w_{yx}(t) = \frac{r_x(t) - s_x(t)}{s_y(t)} \quad (7)$$

$s_{x/y}$ is the symbol transmitted with polarization x and y. $r_x(t)$ is the symbol received.

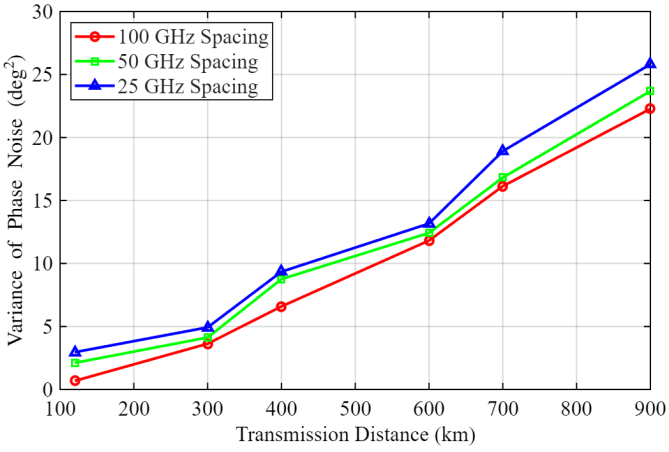

Fig. 3. Phase noise variance on x polarization.

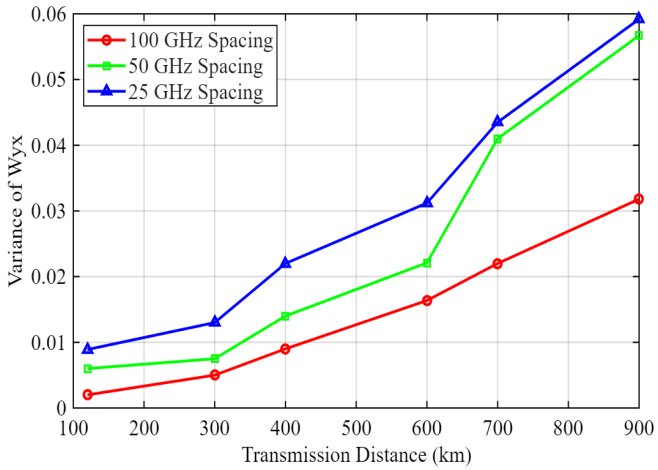

Fig. 4. Variance of polarization crosstalk as a result of XPM.

Figures 3 and 4 show the measured phase-noise and crosstalk variances resulting from XPM over transmission distances of 100km to 900km. Figures 3 and 4 show that the impact of XPM becomes more pronounced as channels are more densely packed and as signals are transmitted over longer distances.

B. Effect of Relative Polarization Rotation on XPM

The findings depicted in Figures 3 and 4 are obtained when all the co-propagating channels are aligned to the same polarization. Figures 5 and 6 show the measured crosstalk and phase noise variances as the relative polarization rotation between the interfering channels and the probe channel is varied. It can be observed that the phase noise variance resulting from XPM reaches its maximum at 45°, and the XPM crosstalk variance is maximized at 0° of polarization rotation.

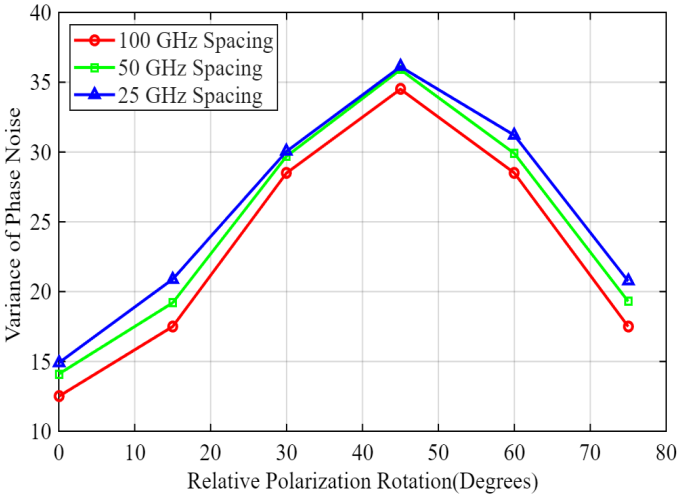

Fig. 5. Influence of relative polarization rotation on phase noise.

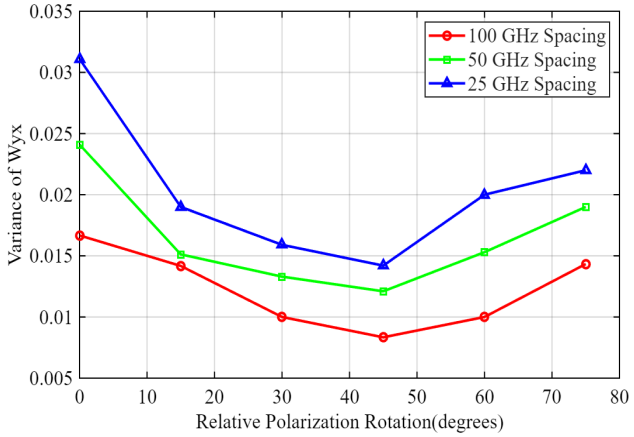

Fig. 6. Influence of relative polarization rotation on polarization crosstalk.

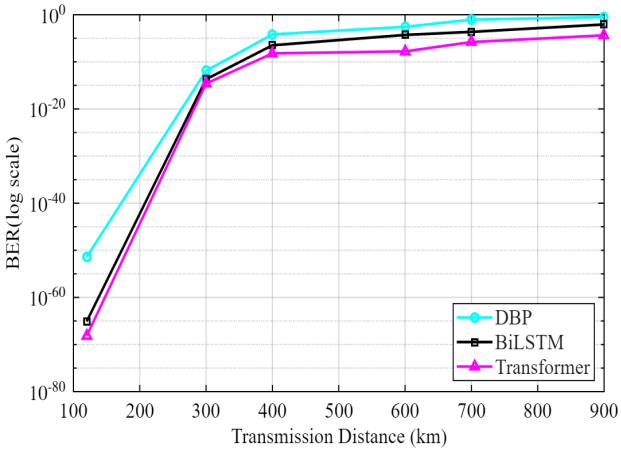

Fig. 7. Performance comparison between DBP, BiLSTM, and transformer models.

C. *Mitigation of Nonlinear Effects*

In this study, the emphasis is on alleviating not only XPM but also all other nonlinear effects. The effectiveness of state-of-the-art DBPs is constrained by computational overhead and the need for high sampling rates, making real-time processing more complex for long-haul transmission. In this study, Transformer and BiLSTM machine learning models are used to alleviate nonlinear effects. The symbols transmitted by the DP-QPSK transmitter block, as depicted in Figure 2, serve as the target symbols for the ML model. At the output of the DSP on the receiver side, I and Q components are captured as a two-dimensional vector. Then the ML model is trained with these components. This DSP includes resampling, QI compensation, CD compensation, FO estimation, AE, and carrier phase recovery, excluding nonlinearity compensation.

Tables II and III show the BiLSTM and transformer parameters, respectively. The performance of the ML models in mitigating nonlinear effects is compared with that of DBP in Figure 7. The results show that the transformer achieves the best BER performance compared with DBP and BiLSTM. The transformer architecture used has 2 heads and 1 encoder layer, with a sequence length of 82.

TABLE II. BI-LSTM PARAMETERS

Parameter	Value
No. of bidirectional layers	2
Optimizer	Adam
No. of units per layer	4 & 50

TABLE III. TRANSFORMER PARAMETERS

Parameter	Value
Feed forward	1024
Feature Size	32
No. of encoder layers	1
No. of fully connected layers	2
Sequence length	82
No. of heads	2
Drop out	0.1

The Bi-LSTM model processes sequential data by taking as input a window of past and future symbols to predict and correct distortions in the current symbol. Although it may not outperform the transformer, it has achieved a lower BER than DBP. The data rate is 28 Gbaud, and the modulation scheme is DP-QPSK. If higher-order modulation schemes are used at higher bitrates, the implementation complexity of the ML techniques would increase. DBP relies heavily on accurate parameter estimation, making it sensitive to variations in fiber characteristics and optical power levels. Because it is a data-driven model, Bi-LSTM learns robust nonlinear mappings but requires extensive retraining when deployed in new environments. Transformers demonstrate greater adaptability by extracting hierarchical features and leveraging global dependencies within the input sequence.

V. CONCLUSION

Cross-Phase Modulation (XPM) is the dominant nonlinear effect for multichannel transmission systems. The study investigated the impact of XPM on a multichannel, 112Gbps coherent Dual-Polarization Quadrature Phase-Shift Keying (DP-QPSK)-based Dense Wavelength Division Multiplexing (DWDM) system used in current optical fiber communication systems in Metropolitan Area Networks and Long-haul networks. In the study, the phase noise and polarization crosstalk were measured. Also, the dependence of the statistical characteristics of XPM on the relative polarization states of the co-propagating channels is verified. The results obtained justified the detrimental effects of XPM on system performance and the dependence of XPM impact on transmission distance and channel spacing. The novelty of this research lies in applying Machine Learning (ML) models to mitigate nonlinear effects in a multichannel optical communication system. Bidirectional Long Short-Term Memory (Bi-LSTM) and transformer ML models were incorporated at the receiver to alleviate the nonlinear effects. The performance of these ML techniques was compared with that of the Digital Back Propagation (DBP) algorithm across transmission distances from 100km to 900km. The results show that ML techniques offer a promising approach to alleviating nonlinear effects in multichannel systems. The Bit

Error Rate (BER) results show that the transformer model outperformed both DBP and Bi-LSTM. Maximum Q factor gain of 1.2dB was observed at a distance of 120km. Future work should explore the effectiveness of the Transformer model with varying hyperparameters: window sizes, Feature dimensions, and feedforward dimensions.

REFERENCES

[1] L. Li *et al.*, "Nonlinear Polarization Crosstalk Canceller for Dual-Polarization Digital Coherent Receivers," in *Optical Fiber Communication Conference (2010), paper OWE3*, Mar. 2010, Art no. OWE3, https://doi.org/10.1364/OFC.2010.OWE3.

[2] Z. Tao *et al.*, "Simple Fiber Model for Determination of XPM Effects," *Journal of Lightwave Technology*, vol. 29, no. 7, pp. 974–986, Apr. 2011, https://doi.org/10.1109/JLT.2011.2107728.

[3] E. Morsy, H. A. Fayed, A. Abd El Aziz, and M. H. Aly, "SPM and XPM crosstalk in WDM systems with DRA: Channel spacing and attenuation effects," *Optics Communications*, vol. 417, pp. 79–82, June 2018, https://doi.org/10.1016/j.optcom.2018.02.028.

[4] J. Ding *et al.*, "Influence of equalization enhanced phase noise on digital nonlinearity compensation in Nyquist-spaced superchannel transmission systems," in *Semiconductor Lasers and Applications XI*, Oct. 2021, vol. 11891, pp. 38–45, https://doi.org/10.1117/12.2600923.

[5] C. Li *et al.*, "Inter-Channel Fiber Nonlinearity Mitigation in High Baud-Rate Optical Communication Systems," *Journal of Lightwave Technology*, vol. 39, no. 6, pp. 1653–1661, Mar. 2021, https://doi.org/10.1109/JLT.2020.3042671.

[6] H. Rabbani, H. Hosseinianfar, H. Rabbani, and M. Brandt-Pearce, "Analysis of Nonlinear Fiber Kerr Effects for Arbitrary Modulation Formats," *Journal of Lightwave Technology*, vol. 41, no. 1, pp. 96–104, Jan. 2023, https://doi.org/10.1109/JLT.2022.3213182.

[7] Z. Tao, W. Yan, S. Oda, T. Hoshida, and J. C. Rasmussen, "A simplified model for nonlinear cross-phase modulation in hybrid optical coherent system," *Optics Express*, vol. 17, no. 16, pp. 13860–13868, Aug. 2009, https://doi.org/10.1364/OE.17.013860.

[8] M. Winter, C.-A. Bunge, D. Setti, and K. Petermann, "A Statistical Treatment of Cross-Polarization Modulation in DWDM Systems," *Journal of Lightwave Technology*, vol. 27, no. 17, pp. 3739–3751, Sept. 2009, https://doi.org/10.1109/JLT.2009.2025394.

[9] Y.-T. Hsueh *et al.*, "Passband Narrowing and Crosstalk Impairments in ROADM-Enabled 100G DWDM Networks," *Journal of Lightwave Technology*, vol. 30, no. 24, pp. 3980–3986, Sept. 2012, https://doi.org/10.1109/JLT.2012.2208262.

[10] M. Seifouri, M. M. Karkhanehchi, and S. Rohani, "Design of Multi-Layer Optical Fibers with Ring Refractive Index to Reduce Dispersion and Increase Bandwidth in Broadband Optical Networks," *Engineering, Technology & Applied Science Research*, vol. 2, no. 3, pp. 216–220, June 2012, https://doi.org/10.48084/etasr.166.

[11] S. Ilic, B. Jaksic, M. Petrovic, A. Markovic, and V. Elcic, "Analysis of Video Signal Transmission Through DWDM Network Based on a Quality Check Algorithm," *Engineering, Technology & Applied Science Research*, vol. 3, no. 2, pp. 416–423, Apr. 2013, https://doi.org/10.48084/etasr.293.

[12] S. Zhang *et al.*, "Field and lab experimental demonstration of nonlinear impairment compensation using neural networks," *Nature Communications*, vol. 10, no. 1, July 2019, Art. no. 3033, https://doi.org/10.1038/s41467-019-10911-9.

[13] A. Singh, N. Gautam, B. Lall, and A. Choudhary, "Restricted Boltzmann Machine Classifier for Nonlinear Compensation in DP-16QAM Single and WDM Coherent Optical Communication Systems," in *2023 Conference on Lasers and Electro-Optics Europe & European Quantum Electronics Conference (CLEO/Europe-EQEC)*, June 2023, https://doi.org/10.1109/CLEO/Europe-EQEC57999.2023.10231617.

[14] E. Giacoumidis, A. Tsokanos, M. Ghanbarisabagh, S. Mhatli, and L. P. Barry, "Unsupervised Support Vector Machines for Nonlinear Blind Equalization in CO-OFDM," *IEEE Photonics Technology Letters*, vol. 30, no. 12, pp. 1091–1094, June 2018, https://doi.org/10.1109/LPT.2018.2832617.

[15] E. Giacoumidis, A. Matin, J. Wei, N. J. Doran, and X. Wang, "Unsupervised Hierarchical Clustering for Blind Nonlinear Equalization in WDM Coherent Optical OFDM," in *Asia Communications and Photonics Conference (2017),* Nov. 2017, Art. no. Su4C.4, https://doi.org/10.1364/ACPC.2017.Su4C.4.

[16] N. Gautam, S. V. Pendem, B. Lall, and A. Choudhary, "Transformer-Based Nonlinear Equalization for DP-16QAM Coherent Optical Communication Systems," *IEEE Communications Letters*, vol. 28, no. 3, pp. 577–581, Mar. 2024, https://doi.org/10.1109/LCOMM.2023.3344996.

[17] S. Goossens *et al.*, "On Fiber Nonlinearity Mitigation via 4D Geometric Shaping for Next-Generation Single-Span Systems," *IEEE Photonics Technology Letters*, vol. 37, no. 6, pp. 349–352, Mar. 2025, https://doi.org/10.1109/LPT.2025.3544404.